Measurement of the Ginzburg-Landau parameter $\kappa_2(T)$ for polycrystalline $YBa_2Cu_3O_{7-\delta}$

H. Zhou, J. Rammer, P. Schleger, W. N. Hardy, and J. F. Carolan
Physics Department, University of British Columbia, Vancouver, British Columbia, Canada V6T 2A6
(Received 5 July 1990)

We have carried out a detailed study of the reversible magnetization of polycrystalline $YBa_2Cu_3O_{7-\delta}$ near T_c in fields H up to 5 T. The magnetization curves at high fields can be fit to the linearized anisotropic Ginzburg-Landau model for nearly randomly oriented grains, and the approximate orientation distribution is obtained. The fit also allows one to extract a number of physical quantities, in particular the critical fields and the generalized Ginzburg-Landau parameter κ_2 near T_c. Both $H_{c2}^{\min}$ and $\kappa_2^{\min}$ (referring to grains with $\hat{\mathbf{c}} \parallel \mathbf{H}$) are enhanced over their mean-field values by a common temperature-dependent factor just below T_c, which implies that H_c is *linear* in temperature up to at least 0.5 K below T_c. At slightly lower temperatures, $\kappa_2^{\min}$ develops a negative slope, as expected from (isotropic) Bardeen-Cooper-Schrieffer theory; however, the temperature dependence is much stronger than predicted.

I. INTRODUCTION

Key features of the macroscopic magnetic behavior of high-T_c superconductors are quite consistent with conventional phenomenological models for type-II superconductors. For example, anisotropic London and Ginzburg-Landau theories[1,2] have been successfully employed to analyze the angular-dependent behavior of the critical fields,[3-5] the London penetration depth,[6,7] and the field-induced torque.[8] Measurements of the magnetization, however, are generally difficult to analyze in terms of intrinsic, equilibrium properties that characterize the ideal material. These non-equilibrium effects, which are due to flux pinning and flow, cause the magnetization to be irreversible and time dependent in an external field. The intrinsic magnetization of high-T_c superconductors is directly measurable only at high temperatures and high fields, where flux-pinning effects become negligible. In this regime, magnetization curves are reversible.[9]

In the present paper we are interested in the equilibrium magnetization of polycrystalline $YBa_2Cu_3O_{7-\delta}$ near T_c in fields close to the upper critical field H_{c2}. Measurements of the magnetization in this region have been reported previously,[9-11] however, these authors concentrated on different aspects as compared to our work. In addition to the fact that the magnetization is reversible, another convenient feature appears in the regime near H_{c2}: the Ginzburg-Landau equations can be linearized due to the smallness of the order parameter. The linearized anisotropic Ginzburg-Landau theory for an arbitrarily oriented single crystal predicts a magnetization which is *linear* in the applied field.[2] In fact, for a high-κ superconductor (κ is the usual Ginzburg-Landau parameter) such as $YBa_2Cu_3O_{7-\delta}$, this linear regime extends to quite low fields on the scale set by (the angular-dependent) H_{c2}.[12] Full high-field magnetization curves for a high-T_c polycrystal consisting of randomly oriented grains were calculated recently[13] using the single-crystal results[2] (for earlier work, see Kogan and Clem[14]). In Sec. III, the relevant equations are reproduced, also taking into account possible deviations from a random orientation distribution of the single-crystalline grains.

Our main objective here is to extract the generalized Ginzburg-Landau parameter κ_2 from our measurements, and establish its temperature dependence near T_c. This parameter is conventionally used to describe the magnetization of a type-II superconductor near the upper critical field at all temperatures. At T_c, κ_2 is by definition identical to the usual Ginzburg-Landau parameter κ. At lower temperatures, Bardeen-Cooper-Schrieffer (BCS) theory predicts a distinct temperature dependence, which is strongly affected by impurity scattering,[15,16] anisotropy[17,18] and strong-coupling effects.[18-20] In view of the absence of theoretical predictions for κ_2 based on alternative models for high-T_c superconductors, we can only compare the results of our analysis with BCS theory. It should, however, be noted that even in this case the theory is not complete, since the anisotropy of $YBa_2Cu_3O_{7-\delta}$ has to our knowledge not yet been taken into account in a satisfactory manner for an arbitrarily oriented crystal.[18]

II. EXPERIMENTAL DETAILS

The experiment was carried out by measuring the magnetic moment of a polycrystalline $YBa_2Cu_3O_{7-\delta}$ sample as a function of magnetic field for different temperatures near T_c. The sample was a small rectangular piece with dimension $0.96 \times 1.65 \times 3.50$ mm^3, cut from a 0.96-mm-thick disk. The disk was pressed from fine-grained powder prepared with the standard method[21] followed by annealing in a flowing oxygen furnace to obtain full

oxygenation. (In our sample the oxygen content is estimated to be 6.987.) Powder x-ray diffraction of another piece from the same disk was consistent with the standard diffraction pattern of a compound of this stoichiometry, without showing any detectable impurity phases.

A superconducting quantum interference device (SQUID) magnetometer manufactured by Quantum Design Inc. was used in this measurement. Two orientations of the sample with respect to the applied magnetic field were investigated. In orientation I the field was perpendicular to the original sample disk plane, that is, parallel to the direction of applied pressure when the $YBa_2Cu_3O_{7-\delta}$ powder was pressed into a disk. In orientation II the field was perpendicular to the pressure direction. Two different clean quartz tubes were used as sample holders for the two orientations. The sample was oriented inside the quartz tube by eye and tightly plugged by quartz wool in order to prevent possible movement during the measurement. A field-cooled susceptibility measurement in orientation II at 10 G indicated an onset of superconductivity around 93 K, and a Meissner fraction of 25%. The plateau was reached at about 87 K.

The magnetic moment was measured in the magnetometer by moving the sample up in discrete steps through a superconducting pickup coil array, which is arranged as a second-order gradiometer. The induced supercurrent in the coils was detected by an rf SQUID and the voltage signal output from the SQUID was recorded as a function of sample position. A linear drift term was subtracted from the voltage signal from such a scan, and the magnetic moment calculated by fitting the corrected voltage signal to the expected pattern of a second-order gradiometer. (This fitting procedure gave an improved signal-to-noise ratio over the manufacturer supplied programs.) For magnetic moments above 10^{-4} emu, the uncertainty of this method of data interpretation was typically 1% to 2% of the calculated moment, and for moments below 10^{-4} emu, the uncertainty was at the noise level of the apparatus, which was about 10^{-6} emu. For each field and temperature point, this scan was repeated eight times. The magnetic moment values calculated for each individual scan was then investigated, and occasionally one or two scans were discarded because the calculated moment values were significantly different from the rest of the scans in the set. Usually these erroneous results came from the first scans after the field change, and were associated with large distortions of the SQUID voltage pattern which we believe was caused by flux creeping in the superconducting magnet after the change of magnetic field. The final results were obtained by averaging the moment values of the scans for the same field and temperature.

The experiment consisted of two series of $m(H)$ measurements (m is the magnetic moment) for the two orientations. In each series, the measurements were performed at constant temperature and varying field. For each $m(H)$ measurement, we set the magnetometer to the desired temperature and waited for two hours to guarantee the temperature stability to be better than 5 mK. After each change of magnetic field, we waited for another 8 minutes before scanning the sample, to avoid the most serious drift period. The field was increased in steps of 0.1 or 0.2 T until the maximum value (usually 5 T) was reached, and then decreased in larger steps to check the reversibility. Within the temperature and field ranges studied, the reversibility was found to be very good (the data were in most cases only slightly above the uncertainty margin of the data fitting in increasing field). However, the error bars for the decreasing field runs tended to be larger than for the increasing field runs, suggesting that for high precision measurements longer waiting times are necessary for larger magnetic field changes. Also we repeated the experiments for some of the $m(H)$ curves to confirm the reliability of this technique, and the results essentially overlapped the previous measurements, within the uncertainty of data interpretation.

The influence of the quartz sample holder signal was checked by measuring the empty holder plus the quartz wool with exactly the same conditions as those with the sample. Within the temperature range of our experiment, 89–95 K, there was no observable temperature dependence of the diamagnetic sample holder signal. The SQUID voltage data of the sample holder, as a function of sample position, was subtracted from those with the sample, and the differences were analyzed by the method discussed above. For all our $m(H)$ curves, the effect of this correction was found to be equivalent to subtracting from the original $m(H)$ curve a straight line, i.e., a diamagnetic signal, plus a small offset. As will be discussed later, this sample-holder correction is irrelevant for our purpose.

III. ANISOTROPIC GINZBURG-LANDAU THEORY FOR A POLYCRYSTAL

Using the linearized anisotropic Ginzburg-Landau (GL) theory, Kogan and Clem[2] have calculated the magnetization near the upper critical field for a uniaxial superconductor oriented arbitrarily in an external field H. For a Ginzburg-Landau parameter $\kappa \gg 1$, their result for the magnetization component parallel to the applied field can be written as follows:

$$-4\pi\mathcal{M}_{\parallel} = \frac{H_{c2}(\theta) - H}{2\beta_A \kappa_2^2(0)}(\cos^2\theta + \epsilon \sin^2\theta). \tag{1}$$

Here

$$H_{c2}(\theta) = \frac{H_{c2}(0)}{\sqrt{\cos^2\theta + \epsilon \sin^2\theta}} \tag{2}$$

and θ is the angle between the crystal symmetry axis ($\hat{c}$) and the direction of the applied field H. In the field regime near H_{c2}, the vortices are parallel to the applied field, and Abrikosov's structure parameter $\beta_A = 1.1596...$, is independent of θ.[13,22] $\kappa_2(0)$ is the generalized GL parameter for $\theta = 0$, equal to $\kappa(0)$ at T_c.

The parameter $\epsilon = M_1/M_3$ is the ratio of the effective masses for charge carriers propagating in the plane and perpendicular to the plane, respectively. For a layered superconductor considered here, $\epsilon < 1$; specifically, from the measured anisotropy of the critical field slopes[4] $[H'_{c2}(\pi/2)/H'_{c2}(0) \sim 5.5]$ for $YBa_2Cu_3O_{7-\delta}$ one finds $\epsilon \sim (1/5.5)^2 \sim \frac{1}{30}$.

For convenience, we will alternatively employ the following notation for the angular-dependent quantities H_{c2} and κ_2:

$$H_{c2}(0) = H_{c2}^{\min}, \quad H_{c2}(\pi/2) = H_{c2}^{\max} = H_{c2}^{\min}/\sqrt{\epsilon},$$

$$\kappa_2(0) = \kappa_2^{\min}, \quad \kappa_2(\pi/2) = \kappa_2^{\max} = \kappa_2^{\min}/\sqrt{\epsilon}.$$

Using the above single-crystal result, it is straightforward to compute the magnetization of a polycrystal consisting of randomly oriented grains whose individual magnetization curves obey Eq. (1).[13] If the orientation distribution is not entirely random, additional contributions to the result derived in Ref. 13 will appear. From the way our sample was prepared (see Sec. II), we expect that a small fraction of the grains will be oriented with their crystallographic $\hat{\mathbf{a}}$, $\hat{\mathbf{b}}$ or $\hat{\mathbf{c}}$ axes perpendicular to the original disk plane, that is, along the direction the pressure was applied. Let f_1 be the fraction of the grains with $\hat{\mathbf{c}}$ perpendicular to the original disk plane and f_2 the fraction with $\hat{\mathbf{a}}$ or $\hat{\mathbf{b}}$ perpendicular to the original disk plane ($\hat{\mathbf{a}}$ and $\hat{\mathbf{b}}$ are taken to be equivalent). Then the magnetization for the two orientations I ($\mathbf{H} \perp$ original disk plane) and II ($\mathbf{H} \parallel$ original disk plane) is, respectively, given by ($f_r = 1 - f_1 - f_2$ is the fraction of randomly oriented grains):

$$\mathcal{M}_{\mathrm{I}} = f_r\mathcal{M}_r + f_1\mathcal{M}_1 + f_2\mathcal{M}_2, \tag{3}$$

$$\mathcal{M}_{\mathrm{II}} = f_r\mathcal{M}_r + f_1\mathcal{M}_2 + f_2\mathcal{M}_3, \tag{4}$$

with

$$-4\pi\mathcal{M}_r = \frac{1}{2\beta_A\kappa_2^2(0)}\left\{H_{c2}\left(\frac{\pi}{2}\right)\left[\frac{\epsilon}{\sqrt{\bar{\epsilon}}}\frac{1}{2}\left(\cos\theta_0\sqrt{\bar{\epsilon}+\cos^2\theta_0} + \bar{\epsilon}\,\mathrm{arcsinh}\frac{\cos\theta_0}{\sqrt{\bar{\epsilon}}}\right)\right] - H\left(\frac{\cos^3\theta_0}{3}(1-\epsilon) + \epsilon\cos\theta_0\right)\right\}, \tag{5}$$

$$-4\pi\mathcal{M}_1 = \frac{H_{c2}(0) - H}{2\beta_A\,\kappa_2^2(0)}, \tag{6}$$

$$-4\pi\mathcal{M}_2 = \epsilon\,\frac{H_{c2}(\pi/2) - H}{2\beta_A\,\kappa_2^2(0)}, \tag{7}$$

$$-4\pi\mathcal{M}_3 = \frac{1}{2\beta_A\kappa_2^2(0)}\left\{H_{c2}(0)\frac{2}{\pi}\left[E\left(\frac{\pi}{2}\backslash\arcsin\sqrt{1-\epsilon}\right) - E(\theta_0\backslash\arcsin\sqrt{1-\epsilon})\right] - H\,\frac{1+\epsilon}{2}\,\frac{\pi - 2\theta_0 - \sin 2\theta_0}{\pi}\right\}. \tag{8}$$

Here

$$\bar{\epsilon} = \frac{\epsilon}{1-\epsilon},$$

and

$$\theta_0 = \arccos\left\{\frac{\epsilon}{1-\epsilon}\left[\left(\frac{H_{c2}(\pi/2)}{H}\right)^2 - 1\right]\right\}^{1/2} \quad \text{for } H > H_{c2}(0)$$

$$= 0 \quad \text{for } H \le H_{c2}(0). \tag{9}$$

The symbol $E(\phi\backslash\alpha)$ is the elliptic integral of the second kind in the notation of Ref. 23. Equation (5) for the contribution from randomly oriented grains was obtained by averaging the single-crystal result (1) over all orientations in space. The expression (8) for $\mathcal{M}_3$ was obtained by averaging the single-crystal magnetization over all orientations with $\hat{\mathbf{c}}$ in the original disk plane, so that either $\hat{\mathbf{a}}$ or $\hat{\mathbf{b}}$ is perpendicular to this plane. This term, which describes a magnetization curve similar to Eq. (5), contributes only to $\mathcal{M}_{\mathrm{II}}$ (orientation II), where the applied field is parallel to the original disk plane. (In orientation I, these grains display a magnetic behavior discribed by $\mathcal{M}_2$.) The "cutoff angle" θ_0, which varies between 0 and $\pi/2$, defines the critical angle θ discriminating differently oriented grains whose individual H_{c2} (θ) is above ($\theta > \theta_0$) and below ($\theta < \theta_0$) the applied field H. If $H \le H_{c2}(0)$, the minimum upper critical field, all grains are superconducting, and $\theta_0 = 0$. Only in this field regime is the total magnetization of a polycrystal, in the framework of the linearized theory, in fact linear in H. Finally, it should be mentioned that demagnetization effects are negligible in the present field range, because the magnetization is very small.

IV. EXPERIMENTAL RESULTS AND FIT TO THE THEORY

In this section we will discuss our experimental results and fit the data to the theory outlined above. Figure 1(a) shows the raw data for several temperatures around T_c, measured in sample orientation I (where the field was applied perpendicular to the original disk plane). The maximum scatter in the data is approximately 10^{-6} emu, which is smaller than $\frac{1}{10}$ the size of the symbols. The linear dependence of the magnetic moment on the field for the temperatures $92-95$ K indicates that we are looking at the normal state, with signs of superconductivity appearing below 1 T at 92 K. The nonzero and temperature-dependent slopes of the dashed lines in Fig. 1(a) are due to the competing influences from a sizable paramagnetic contribution and diamagnetic (superconducting) fluctuations, including also a temperature-independent contribution from the sample holder (see Sec. II).

Figure 1(a) also shows six magnetization curves below T_c, for temperatures between 89.0 and 91.5 K. The vertical arrows mark the fields $H_{c2}(0)=H_{c2}^{\min}$, below which a careful analysis reveals a narrow linear regime. This linear regime occurs due to the fact that, below $H_{c2}^{\min}$, all (potentially superconducting) grains are in the superconducting state, and that the field is still high enough for the linearized theory to hold (at least for the majority of the grains). At fields exceeding $H_{c2}^{\min}$, more and more grains are driven normal according to their orientation in the field, yielding a nonlinear total magnetization. Also, the linear regime below $H_{c2}^{\min}$ is expected to eventually give way to a regime exhibiting a progressively more pronounced downward curvature in the magnetization at lower fields, indicative of the breakdown of the linearized theory. The linear portion is indicated for exemplary purposes by the 90.5-K curve.

The exact position of the vertical arrows which mark the upper end of the linear regime ($H_{c2}^{\min}$) was determined in a systematic way as follows. In Fig. 1(b) we have differentiated the magnetization curves of Fig. 1(a) with respect to the field. The narrow linear regime shows up in the differentiated curves as characteristic shoulders which we use to identify $H_{c2}^{\min}$. The dashed curves in Fig. 1(b) are extrapolations from the high-field regime to fields below $H_{c2}^{\min}$. The arrows indicate these characteristic fields. One can see that the identification of $H_{c2}^{\min}$ is not always unambiguous, in particular with the 90.0-K curve; to be specific, for this temperature we have chosen $H_{c2}^{\min}=3.3$ T in the subsequent further evaluation of our data. (The temperature dependence of $H_{c2}^{\min}$ will be discussed later.)

Figure 1(c) shows our data for the magnetic moment for the same temperatures below T_c as before, for sample orientation II (see Sec. II). We observe qualitatively the same features as with orientation I, apart from a different linear background due to a different sample holder which had to be used for technical reasons. Furthermore, since the statistics for orientation II was not as good as with the previous measurement, it is very difficult to deter-

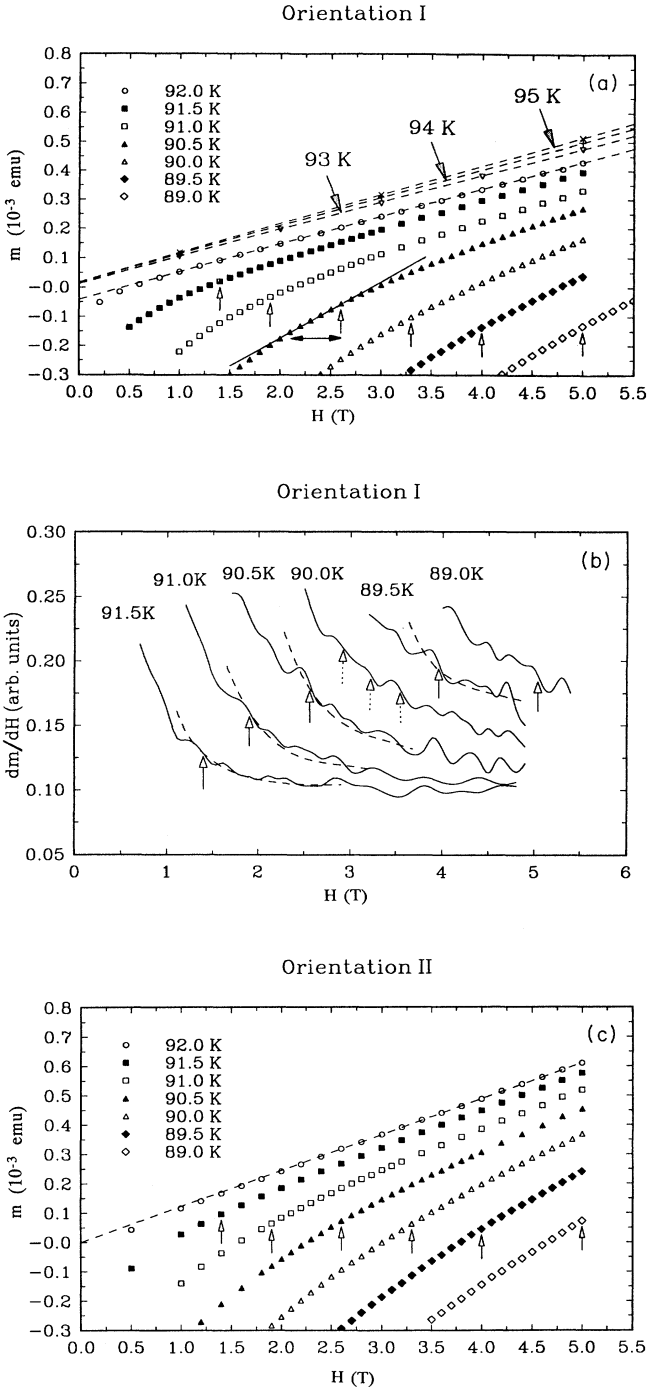

FIG. 1. (a) Measured magnetic moment as a function of applied field for several temperatures above and below T_c for sample orientation I (see Sec. II). The error bars are smaller than $\frac{1}{10}$ the size of the symbols. The vertical arrows indicate the critical fields $H_{c2}^{\min}$ as obtained from (b) The dashed lines emphasize the linear behavior above T_c. (b) Differentiated data from (a) for the determination of $H_{c2}^{\min}$ (arrows). The dashed lines are approximate extrapolations from the high-field regime to fields below $H_{c2}^{\min}$. The broken arrows indicate uncertainties in the definition of $H_{c2}^{\min}$ for the 90.0-K curve. (c) Same as (a), for orientation II (see Sec. II).

mine the fields $H_{c2}^{\min}$ in the same way as before. Also, as can be seen by carefully comparing Fig. 1(a) with Fig. 1(c), the kink for the second sample orientation is slightly less pronounced. This will be attributed later in this section to a small deviation from a random orientation distribution of the grains, consistent with the way the sample was prepared. For these reasons, we have decided to employ the values for $H_{c2}^{\min}$ determined in the previous analysis [Fig. 1(b)]; they are consistent with the data in Fig. 1(c), as expected.

We now proceed to the discussion of our fit procedure using the theory summarized in Sec. III. In order to obtain from our data the bare magnetic moment of the sample due to the vortex state alone, the background magnetization originating from three contributions has to be subtracted from the measured signal. These three contributions are the paramagnetic moment due to nonsuperconducting phases, the (superconducting) diamagnetic fluctuation contribution, and the signal from the sample holder. The first two contributions are certainly temperature dependent. The signal from the empty sample holder including the quartz wool was determined in Sec. II to be linear in the field, with a small nonzero offset at $H=0$; no significant temperature dependence of the sample holder signal could be detected.

In order to assess the field and temperature dependence of the magnetic moment due to the full background, we go back to Fig. 1(a) and consider the magnetization curves for the temperatures 92 – 95 K. These curves suggest that the magnetization above (the zero-field) T_c ($\simeq$ 92.1 K), including the sample holder contribution, is of the form $a(T)+b(T)\,H$, with temperature-dependent coefficients a and b. In particular the offset a obviously develops a strong temperature dependence below about 93 K, because of enhanced diamagnetic fluctuations. It is expected that this trend continues below the zero-field T_c, due to the finite transition width of the Meissner signal observed in our sample (Sec. II). Furthermore, superconducting grains will tend to induce or enhance, via proximity effect, diamagnetic fluctuations in adjacent, nonsuperconducting grains. It is therefore tempting to assume a magnetic background of the same linear form as observed above 92 K, also for temperatures where some of the grains exhibit a vortex state. We will show in the following that with this assumption, it is indeed possible to obtain an excellent fit of our data to the linearized Ginzburg-Landau theory outlined in Sec. III.

The bare experimental magnetization due to the vortex state alone is thus given by the following expression:

$$\mathcal{M}_{\text{expt}} = \frac{m(T,H) - a(T) - b(T)\,H}{V}, \qquad (10)$$

with $m(T,H)$ the measured magnetic moment of the sample including the signal from the sample holder [Figs. 1(a) and 1(c)], and a and b temperature-dependent coefficients to be determined from a fit to the theory; V is the real superconducting volume as obtained from the sample dimensions, its weight, and the low-field Meissner signal. For our sample, $V=1.03\times10^{-3}$ cm^3.

Equation (10) for the two sample orientations has to be fit to the theoretical magnetization curves Eqs. (3) and (4) for orientations I and II, respectively. It turns out that if we assume a random orientation distribution of the grains [$f_1=f_2=0$ in Eqs. (3) and (4)], then only the data for orientation II can be fit in a satisfactory manner. This is understood as follows in terms of a certain degree of alignment of grains. As can be seen from Eq. (4), $\mathcal{M}_{\text{II}}$ contains, apart from the "random" term, two additional contributions arising from grains with their $\hat{\mathbf{c}}$ axes perpendicular to the field ($\mathcal{M}_2$), and randomly distributed in the sample plane along which the field is applied ($\mathcal{M}_3$). The contribution $\mathcal{M}_2$, however, has the same form as the background, and is thus in our analysis absorbed in the fitted coefficients a and b. Also, the contribution $\mathcal{M}_3$ looks (if plotted) somewhat similar to $\mathcal{M}_r$. Therefore, if the total fraction of aligned grains is not too large, the full magnetization for orientation II will resemble the "random" curve, and the fractions f_1 and f_2 cannot be determined. For orientation I, however, the situation is different. Equation (3) for $\mathcal{M}_{\text{I}}$ includes the contribution $\mathcal{M}_1$ from grains with their $\hat{\mathbf{c}}$ axes parallel to the applied field, which cannot be absorbed in the background. This contribution will show up in the measured magnetization as a characteristic distortion of the "random" curve that can be used to determine f_1 from the optimum fit.

Figures 2(a) and 2(b) show the fits for the two sample orientations for all measured temperatures. The theory curves are based on an anisotropy parameter $\epsilon=1/30$.[4] From the best fit for orientation I we obtain $f_1=0.07$ with an estimated uncertainty of about ±0.01. Since we cannot determine f_2 from our analysis, we assume for definiteness that the same fraction of grains is aligned with their $\hat{\mathbf{a}}$ and $\hat{\mathbf{b}}$ axes along the original sample disk axis as is aligned with their $\hat{\mathbf{c}}$ axes. Thus we set $f_2=0.14$; it follows that the fraction of randomly oriented grains $f_r=0.79$. An alternative choice for f_2 does not significantly alter our results, as long as f_2 is still small. From the fact that the fits in Figs. 2(a) and 2(b) work so well we conclude that (i) the assumption of a linear magnetization background is justified and that (ii) the anisotropic Ginzburg-Landau model for polycrystals indeed describes our data.

In Table I, we list the parameters a and b corresponding to the fitted linear magnetization background [Eq. (10)]. As expected, the observed trend in the magnetization above 92 K [Fig. 1(a)] continues below this temperature. Also, our preliminary experiments on oriented grains in epoxy, for $\hat{\mathbf{c}} \parallel \mathbf{H}$, directly reveal a similar linear background above $H_{c2}(T)$, for $T \leq 92$ K. We find that both $a(T)$ and $b(T)$ display qualitatively the same temperature dependence as shown in Table I.

We will now extract, from the above fits, physical parameters characterizing the superconductor. From the scaling factors for the magnetization curves in Figs. 2(a) and 2(b) that were needed in order to match the experimental data with the theory curves we obtain the general-

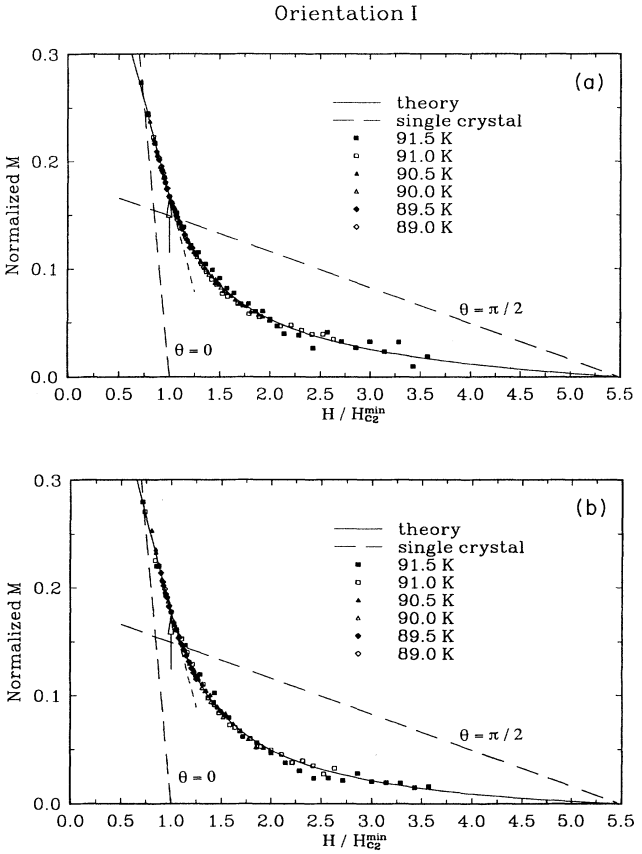

FIG. 2. Normalized magnetization, with extraneous contributions removed, as a function of $H/H_{c2}^{\min}$ as obtained from Fig. 1 employing the fit procedure described in the text. The plotted quantity is $(-4\pi\mathcal{M})2\beta_A(\kappa_2^{\min})^2/H_{c2}^{\min}$. Data points at fields below the linear regime are omitted. The theory curve (solid line) is given by Eq. (3) [Eq. (4)] with $\epsilon = \frac{1}{30}$ and $f_1 = f_2/2 = 0.07$ ($f_r = 0.79$). The scaling factors for the experimental data for each temperature are chosen such that the values at $H/H_{c2}^{\min}$=1 (arrow) match the theory curve. This gives $\kappa_2^{\min}$ (T). (a) Sample orientation I. (b) Sample orientation II.

ized Ginzburg-Landau parameter $\kappa_2^{\min} = \kappa_2(0)$ [see Eqs. (3) and (4)]. Figure 3 shows a plot of $\kappa_2^{\min}$ as a function of temperature for the six temperatures investigated, for both orientations. The small, but apparently systematic discrepancies between the two orientations which are seen in the figure reflect the degree of reliability of our analysis. They may indicate distinctly different temperature effects in the vortex state for grains with their $\hat{\mathbf{c}}$ axes parallel and perpendicular to the field, which are not included in the present Ginzburg-Landau treatment. Since the fraction of oriented grains is small, the discrepancies are not very pronounced.

Figure 3 clearly shows a nonmonotonic temperature dependence of $\kappa_2^{\min}$. We first comment on the upturn for temperatures near T_c. In order to relate this behavior to the temperature dependence of the critical fields near T_c, we have plotted our measured $H_{c2}^{\min}$ [see Fig. 1(b)] in Fig. 4. A similar upward deviation with respect to the mean-field behavior can be seen in these data just below T_c, as also observed in H_{c2} measurements on twinned single crystals.[4] In fact, according to Figs. 3 and 4, these enhancement factors for $H_{c2}^{\min}$ are approximately the same as for $\kappa_2^{\min}$ at each temperature. This implies, using the relation

$$\kappa_2 \simeq \kappa_1 = \frac{H_{c2}}{\sqrt{2}\,H_c} \tag{11}$$

near T_c, that the thermodynamic critical field H_c is approximately *linear* in temperature up to at least 0.5 K below T_c (Fig. 4). An alternative way of visualizing this relationship is to consider the area under the magnetization curve when both $H_{c2}^{\min}$ and $\kappa_2^{\min}$ are enhanced over their mean-field values by the same factor. Since the magnetization slope is proportional to $1/\kappa_2^2$, this area, and therefore H_c, will follow the mean-field behavior as a function of temperature. Using standard thermodynamic relations, the measured slope of H_c gives a value for the (zero-field) specific-heat jump of $\Delta C/T_c = (dH_c/dT)^2/4\pi \simeq 0.056 - 0.065$ J/K^2 mol, in good agreement with directly measured values for $YBa_2Cu_3O_{7-\delta}$ [0.046 J/K^2 mol (Ref. 24), 0.055 J/K^2 mol (Ref. 25), $\leq$ 0.067 J/K^2 mol (Ref. 26)]. Furthermore, from the extrapolated Ginzburg-Landau parameter $\kappa_2^{\min}(T \to T_c) = \kappa^{\min} \simeq 35$ and the H_c slope indicated in Fig. 4, we obtain, using the exact numerical Ginzburg-Landau solution for H_{c1},[27] $dH_{c1}(\theta = 0)/dT = dH_{c1}^{\max}/dT = -2.1$ mT/K. We finally note that our directly measured $H_{c2}^{\min}$ slope in Fig. 4 ($\simeq -1.56$ T/K) is somewhat smaller than the single-crystal result[4] (-1.9 T/K).

Another characteristic feature in Fig. 3 is the negative slope of $\kappa_2^{\min}$ that develops at temperatures below $\sim$ 90 K. A negative slope for κ_2 is expected in the framework of the BCS model, for weak[15,16] and strong coupling,[19,20] isotropic and anisotropic[17,18] superconductors. Also, these theories predict a much larger slope for clean than for dirty superconductors. From Fig. 3, we obtain for the normalized asymptotic slope approximately $(\kappa_2^{\min})' T_c/\kappa \simeq -12$, which is almost ten

TABLE I. Coefficients a and b for the linear magnetization background [see Eq. (10)] for the two sample orientations.

	Orient.	91.5 K	91.0 K	90.5 K	90.0 K	89.5 K	89.0 K
a (memu)	I	−0.049	−0.110	−0.175	−0.270	−0.413	−0.521
a (memu)	II	−0.091	−0.164	−0.223	−0.338	−0.495	−0.590
b (memu/T)	I	0.1275	0.1282	0.1312	0.1392	0.1486	0.1494
b (memu/T)	II	0.0980	0.1018	0.1058	0.1148	0.1280	0.1268

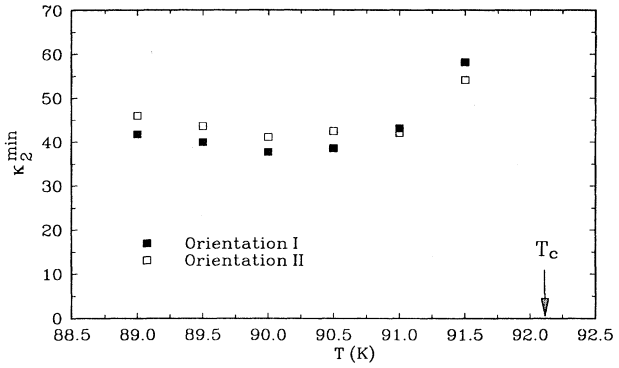

FIG. 3. The generalized Ginzburg-Landau parameter $\kappa_2^{\min}(T)$ as obtained from the fit shown in Fig. 2, for both sample orientations. Note the upturn near T_c.

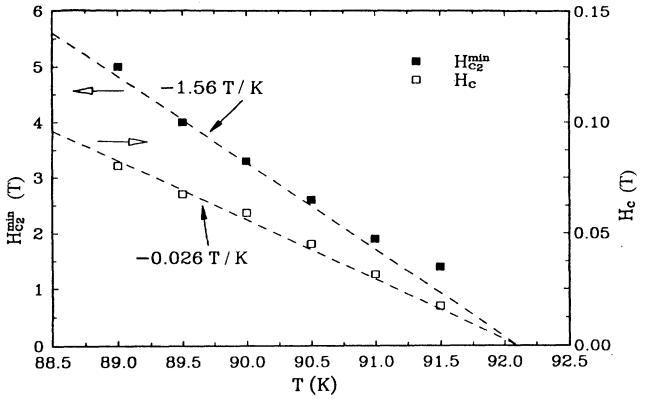

FIG. 4. $H_{c2}^{\min}(T)$ and $H_c(T)$ as obtained from Fig. 1(b) and Eq. (11), respectively. The data for H_c are based on the averaged results for $\kappa_2^{\min}$ for the two sample orientations (Fig. 3). Note the upward curvature of $H_{c2}^{\min}$ near T_c, and the linear behavior of H_c.

times larger than the isotropic, weak-coupling BCS result in the clean limit[15,16] (−1.37). From the above work, however, it is known that both anisotropy and strong-coupling effects can significantly enhance the temperature dependence of κ_2. For instance, the experimental value −2.9 for $(\kappa_2^{\min})' T_c/\kappa$ observed in pure single-crystalline niobium has been quantitatively attributed to Fermi-surface anisotropy and (to a lesser degree) strong-coupling corrections.[17] A recent weak-coupling BCS calculation[18] for a 1:2:3 single crystal with $\hat{\mathbf{c}} \| \mathbf{H}$ however, predicts a somewhat reduced slope, as compared with the isotropic theory. To our knowledge, there exist unfortunately no calculations on the temperature dependence of κ_2 for an arbitrarily oriented layered single crystal. We can therefore not compare our experimental result on κ_2 with a detailed BCS calculation. Also, to our knowledge, there exists no theory of κ_2 based on alternative models for high-T_c superconductors.

V. CONCLUSION

The main results of our extensive study of the *dc* magnetization of a 1:2:3 polycrystal near the upper critical field are the following. Our fitting procedure, which is based on the linearized anisotropic Ginzburg-Landau theory, allows us to determine the fraction of grains in the sample which are oriented with their $\hat{\mathbf{c}}$ axes along the applied field. The quality of the fit is excellent, which suggests that the underlying theory is applicable. In particular, we conclude that in the present regime, Abrikosov's structure parameter β_A is indeed isotropic,[13] and that therefore the vortices are not significantly tilted with respect to the direction of the applied field.

From our analysis we also obtain the minimum upper critical field (referring to grains with $\hat{\mathbf{c}} \| \mathbf{H}$) and the generalized Ginzburg-Landau parameter $\kappa_2^{\min}$ in the temperature regime from 89.0 to 91.5 K. Both quantities are enhanced over their mean-field values in a similar way just below T_c, which indicates a common origin of this effect. It also indicates that the thermodynamic critical field H_c is approximately linear in temperature between 89.0 and 91.5 K. From the obtained well-defined H_c slope, we derive a value for the specific-heat jump $\Delta C/T_c$ which is in very good agreement with recent calorimetric measurements on polycrystals.[26]

Finally, we observe a crossover for $\kappa_2^{\min}$ to a negative slope below ~90 K. The value of the slope is about ten times as large as expected for weak-coupling, isotropic BCS superconductors. Unfortunately, the full BCS calculation including a reliable anisotropy model for arbitrarily oriented grains is not available for comparison. Also, higher fields will be needed in future experiments in order to substantiate the present results regarding the temperature dependence of κ_2.

ACKNOWLEDGMENTS

This work was supported by the Natural Sciences and Engineering Research Council (NSERC) of Canada.

[1]V.L. Ginzburg, Zh. Eksp. Teor. Fiz. **23**, 236 (1952).
[2]V.G. Kogan and J.R. Clem, Phys. Rev. B **24**, 2497 (1981).
[3]T.K. Worthington, W.J. Gallagher, and T.R. Dinger, Phys. Rev. Lett. **59**, 1160 (1987).
[4]U. Welp, W.K. Kwok, G.W. Crabtree, K.G. Vandervoort, and J.Z. Liu, Phys. Rev. Lett. **62**, 1908 (1989).
[5]S. Gygax, W. Xing, O. Rajora, and A. Curzon, Physica C **162-164**, 1551 (1989).
[6]Sreeparna Mitra, J.H. Cho, W.C. Lee, D.C. Johnston, and V.G. Kogan, Phys. Rev. B **40**, 2674 (1989).
[7]E.M. Forgan, S.L. Lee, S. Sutton, J.S. Abell, S.F.J. Cox, C.A. Scott, H. Keller, B. Pümpin, J.W. Schneider, H.

Simmler, P. Zimmermann, and I.M. Savić, in *Proceedings of the 5th International μSR Conference*, Oxford, 1990 [Hyperfine Interact. (to be published)].
[8]D.E. Farrell, J.P. Rice, D.M. Ginsberg, and J.Z. Liu, Phys. Rev. Lett. **64**, 1573 (1990).
[9]For a review on magnetization measurements on high-T_c superconductors, see, e.g., H.W. Weber, in *Studies of High Temperature Superconductors*, edited by A. Narlikar (Nova Science Publishers, New York, 1989), Vol. 3, pp. 197-227.
[10]G. Triscone, A. Junod, and J. Muller, Physica C **162-164**, 470 (1989).
[11]K.S. Athreya, O.B. Hyun, J.E. Ostenson, J.R. Clem, and D.K. Finnemore, Phys. Rev. B **38**, 11 846 (1988).
[12]For a recent numerical solution of the nonlinear Ginzburg-Landau equations, see M.M. Doria, J.E. Gubernatis, and D. Rainer, Phys. Rev. B **41**, 6335 (1990).
[13]J. Rammer (unpublished).
[14]V.G. Kogan and J.R. Clem, Jpn. J. Appl. Phys. **26**, 1159 (1987).
[15]L. Neumann and L. Tewordt, Z. Phys. **191**, 73 (1966).
[16]G. Eilenberger, Phys. Rev. **153**, 584 (1967).
[17]E. Seidl, C. Laa, H.P. Wiesinger, H. W. Weber, J. Rammer, and E. Schachinger, Physica C **161**, 294 (1989).
[18]J. Rammer and W. Pesch, Physica C **162-164**, 205 (1989).
[19]D. Rainer and K.D. Usadel, Phys. Rev. B **9**, 2409 (1974).
[20]J. Rammer and W. Pesch, J. Low Temp. Phys. **77**, 235 (1989).
[21]See, for example, R.F. Kiefl, J.H. Brewer, I. Affleck, J.F. Carolan, P.D. Dosanjh, W.N. Hardy, T. Hsu, R. Kadono, J.R. Kempton, S.R. Kreitsman, Q. Li, A.H. O'Reilly, T.M. Riseman, P. Schleger, P.C.E. Stamp, H. Zhou, L.P. Le, G.M. Luke, B. Sternlieb, Y.J. Uemura, H.R. Hart, and K.W. Lay, Phys. Rev. Lett. **64**, 2082 (1990).
[22]D.R. Tilley, Proc. Phys. Soc. London **85**, 1177 (1965).
[23]M. Abramowitz and I.A. Stegun, *Pocketbook of Mathematical Functions* (Verlag Harri Deutsch, Thun, Frankfurt/Main, 1984), p. 234.
[24]S.E. Inderhees, M.B. Salamon, T.A. Friedmann, and D.M. Ginsberg, Phys. Rev. B **36**, 2401 (1987).
[25]M.V. Nevitt, G.W. Crabtree, and T.E. Klippert, Phys. Rev. B **36**, 2398 (1987).
[26]A. Junod, D. Eckert, T. Graf, G. Triscone, and J. Muller, Physica C **162-164**, 1401 (1989).
[27]J.L. Harden and V. Arp, Cryogenics **3**, 30 (1963).